Intrinsic foot muscles have the capacity to control deformation of the longitudinal arch

Luke A. Kelly[1,2], Andrew G. Cresswell[1], Sebastien Racinais[1,2], Rodney Whiteley[2] and Glen Lichtwark[1]

[1]Centre for Sensorimotor Neuroscience, School of Human Movement Studies, The University of Queensland, Brisbane, Queensland, Australia
[2]Department of Exercise and Sport Science, Aspetar, Qatar Orthopaedic and Sports Medicine Hospital, Doha, Qatar

Research

The human foot is characterized by a pronounced longitudinal arch (LA) that compresses and recoils in response to external load during locomotion, allowing for storage and return of elastic energy within the passive structures of the arch and contributing to metabolic energy savings. Here, we examine the potential for active muscular contribution to the biomechanics of arch deformation and recoil. We test the hypotheses that activation of the three largest plantar intrinsic foot muscles, abductor hallucis, flexor digitorum and quadratus plantae is associated with muscle stretch in response to external load on the foot and that activation of these muscles (via electrical stimulation) will generate sufficient force to counter the deformation of LA caused by the external load. We found that recruitment of the intrinsic foot muscles increased with increasing load, beyond specific load thresholds. Interestingly, LA deformation and muscle stretch plateaued towards the maximum load of 150% body weight, when muscle activity was greatest. Electrical stimulation of the plantar intrinsic muscles countered the deformation that occurred owing to the application of external load by reducing the length and increasing the height of the LA. These findings demonstrate that these muscles have the capacity to control foot posture and LA stiffness and may provide a buttressing effect during foot loading. This active arch stiffening mechanism may have important implications for how forces are transmitted during locomotion and postural activities as well as consequences for metabolic energy saving.

1. Introduction

The human foot is a flexible structure, capable of conforming to variations in surface and load to maintain effective force transmission between the lower limb and the ground. This functionality is achieved via an intricate interaction of movements occurring in a series of small joints, which allows the longitudinal arch (LA) to lengthen and lower during stance [1] and absorb loading forces as elastic strain energy [2,3]. Later in the stance phase, passive elastic recoil of the plantar aponeurosis contributes to positive work generation for propulsion, aided by the windlass mechanism, which effectively stiffens the LA during toe extension [2–4]. This process allows for a highly efficient bipedal gait that is unique to humans [5].

The plantar aponeurosis along with the windlass mechanism is considered the key contributors to foot stiffness during human gait [2,4]. It is proposed that extension of the toes in mid- to late-stance, creates increased tension in the plantar aponeurosis, resulting in shortening of the LA via flexion and adduction of the metatarsals in combination with supination of the rear-foot [4,6]. These alterations in bony alignment act to stiffen the foot and transform it from a compliant attenuator to a rigid lever, allowing ankle plantar flexor torque to be efficiently transmitted to the ground [7]. Recent studies investigating the biomechanics of LA deformation during locomotion have confirmed that the

plantar aponeurosis has a critical influence on the stiffness of the LA [6,8]. However, these studies [8] and others by Pataky *et al.* [9] and Bates *et al.* [10] have also highlighted the potential contribution of an active stiffening mechanism, possibly produced by muscles such as the plantar intrinsic foot muscles.

The plantar intrinsic foot muscles possess origins and insertions that are contained within the foot with the three largest muscles, abductor hallucis (AH), flexor digitorum brevis (FDB) and quadratus plantae (QP), having muscle–tendon units that span the length of the LA [11–13]. The function of these muscles during stance and gait has been the subject of speculation for many years and remains an area of intense interest. Anatomy texts describe these muscles as accessory toe flexors, which may also aid in fore-foot stabilization during the push-off phase of gait [14]. It appears, however, that a disparity exists between the mechanical action proposed by textbooks and the electromyography (EMG) profiles described in the literature. Early EMG studies suggest these muscles may play a role in stabilization of the LA, with muscle recruitment occurring in response to increased loading [15,16]. Further supporting this hypothesis, individuals with a lower LA height in stance (i.e. greater LA deformation) were shown to display greater levels of intrinsic muscle activity [17]. Recent studies from our own laboratory using intramuscular EMG have reported that the plantar intrinsic muscles act in a synchronous manner to provide postural support for the foot, with activation amplitude and timing being correlated with postural task difficulty and medial postural sway, respectively [18].

Despite some evidence suggesting that the plantar intrinsic foot muscles may actively contribute to regulation of foot stiffness during stance and gait [8,9], the specific mechanical functions of these muscles are yet to be described. It is also unknown whether these small muscles are able to generate enough force to produce a significant alteration in foot biomechanics under loaded conditions, in order to influence LA biomechanics. Here, we tested two hypotheses, first, that the LA would deform under increasing load, producing stretch of the plantar intrinsic foot muscles (AH, FDB and QP) and an increase in involuntary activity. Second, we tested the hypothesis that these same muscles are capable of generating sufficient forces to attenuate LA deformation produced by the load, effectively increasing LA stiffness. Activation of these muscles with load and their ability to generate sufficient force to counter LA deformation may have important implications for how the foot can absorb and generate energy during gait.

2. Material and methods

2.1. Participants

Nine healthy males with no history of neuromuscular disorder or lower limb injury in the previous six months volunteered to participate in the study (mean ± standard deviation (s.d.) for age, height and body mass were 30 ± 4 years, 179 ± 7 cm and 80 ± 6 kg, respectively). All participants were informed of the study requirements, benefits and risks before giving written informed consent. The procedures were approved by the local scientific ethics committee and performed according to the Declaration of Helsinki. Two discrete experiments with similar experimental set-ups were performed on the same group of participants during the one test session, in order to address our two hypotheses.
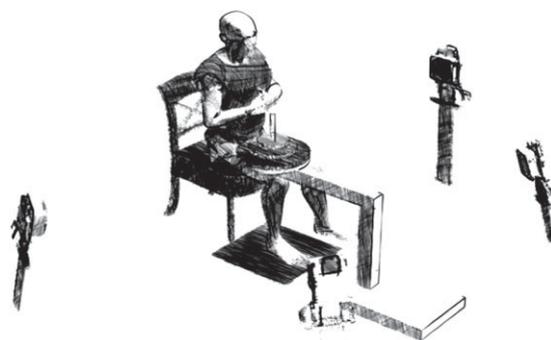
Figure 1. Experimental set-up. Foot motion, ground reaction forces and intramuscular electromyography were recorded during incremental loading (experiment 1) and independent electrically evoked contractions of the three major plantar intrinsic foot muscles (experiment 2). Loads ranging from 0% to 150% of body mass were added to a loading device, which was secured to the distal aspect of the participants right thigh. The participant's foot was placed on the centre of a force plate and four motion analysis cameras were positioned to record three-dimensional motion of the shank and two individual foot segments during each task.

2.2. Experiment 1: foot loading

The aim of this experiment was to examine the relationship between mechanical loading of the foot and both deformation of the foot and also muscle activity of the intrinsic foot muscles (AH, FDB and QP). Loads were incrementally applied to the thigh via a loading rig described in detail below (figure 1). Loads ranged from 0% body mass to 150% body mass with 25% increments. A period of approximately 5 s was maintained at each loading increment, during which time intramuscular EMG, kinematic and force plate data were recorded. Subjects were advised to remain still and refrain from any voluntary movement throughout the trial.

2.3. Experiment 2: electrically evoked muscle contractions

The aim of this experiment was to determine the mechanical response of the foot to stimulation of the individual intrinsic foot muscles (AH, FDB and QP) under different loading conditions. Loads corresponding to 50% and 100% of body mass were applied using the same loading rig described above while each individual muscle was electrically stimulated. One experimental trial consisted of three electrically evoked contractions, each separated by 15 s, for each muscle. The trial was completed for each of the three muscles under the two loading conditions, which were undertaken in a randomized order. As such, a total of six trials were completed for each participant.

2.4. General experimental set-up

Each participant was seated with their right foot placed flat on a marked area in the centre of a force plate (Kistler 9286A, Zurich, Switzerland). The shank was positioned at approximately 10° of flexion (relative to vertical) with the femur positioned parallel to the floor. Loads of up to 150% of body mass could be applied to the distal aspect of thigh using a custom built rig (figure 1), so that the vertical force was located slightly anterior to the ankle joint axis, similar to where it occurs during quiet standing [19].

2.4.1. Muscle activation and stimulation

Paired, fine wire, intramuscular electrodes (0.051 mm stainless steel, Teflon-coated, Chalgren, USA) were inserted into both the proximal and distal ends of the AH, FDB and QP muscles in the right foot (figure 2) of each subject using delivery needles
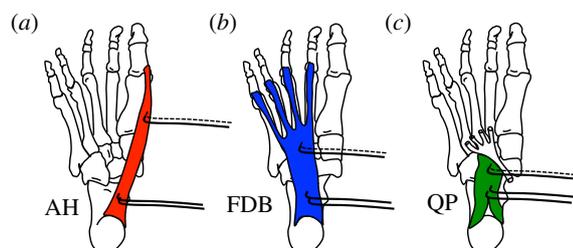
Figure 2. Location of electrodes within the intrinsic foot muscles. Schematic of the anatomical location of (*a*) abductor hallucis (AH), (*b*) flexor digitorum brevis (FDB) and (*c*) quadratus plantae (QP) from the plantar aspect of a right foot. Fine wire pairs of electromyography (EMG) electrodes (black lines with hooked ends) were inserted under ultrasound guidance, with one pair being inserted proximally and one pair distally to the muscle belly. The proximal electrode pair was used for the EMG recordings in experiment 1, whereas one wire from each of the proximal and distal pairs was connected to a constant current electrical stimulator, which delivered trains of electrical stimulation to each muscle independently in experiment 2. (Online version in colour.)

(0.5 × 50 mm) under B-mode ultrasound guidance (12 MHz, 38 mm linear array, Siemens Acuson Antares, USA) [18]. After removal of the delivery needles, the muscles were imaged once more to determine that the ends of the fine wire electrodes remained within the relevant muscle after needle removal. The most proximal pair of fine wire electrodes was used for measuring EMG activity during foot loading (experiment 1 only). The electrodes had a detection length of 2 mm and were separated by approximately 2 mm. A surface ground electrode was attached to the medial malleolus of the right ankle and secured with adhesive tape. All signals were amplified 1000 times, band-pass filtered from 30 Hz to 1 kHz (Delsys Bagnoli, Boston, MA, USA) and subsequently analogue to digitally converted (Power 1401, Cambridge Electronic Design, Cambridge, UK) at a sampling rate of 10 kHz and collected using SPIKE2 software (Cambridge Electronic Design). All data were manually inspected to ensure that muscle electrical activity could be clearly distinguished from that of background noise or artefact. In the case where recordings were contaminated by artefact, or muscle electrical activity appeared absent, the location of the fine wire electrodes was slightly adjusted, and the loading task was repeated. If clear signals could not be obtained following this procedure, then the data from that individual were excluded from further analysis.

For experiment 2, a constant current electrical stimulator (Digitimer DS7AH, Digitmer, Hertfordshire, UK) was connected to one of each pair of intramuscular electrodes with the cathode connected to the proximal electrode and anode to the distal electrode. The electrical stimulator was programmed using SPIKE v. 2 software (Cambridge Electronic Design) to deliver trains of current pulses (400 V, 20 rectangular pulses, 10 μs pulse width, 40 Hz frequency) across the motor point of the muscle. A submaximal level of stimulating current was determined prior to data collection by delivering a train of pulses commencing at 1 mA and increasing incrementally by 1 mA until a mechanical response was observed as a minimum change of 10 N in the vertical ground reaction force. The 10 N vertical force threshold was chosen so as to elicit a clear mechanical response while minimizing subject discomfort. The above task was undertaken with a mass of 20 kg applied to the thigh using the loading rig, in order to ensure consistent foot position on the force plate during the stimulations. Mean stimulation intensities were 6 ± 1 mA for all muscles.

2.4.2. Foot motion and force measurements
Three-dimensional motion capture and force plate data were collected in order to quantify the magnitude and direction of the biomechanical responses owing to loading and/or muscle stimulation. Fourteen retro-reflective markers (diameter 9.0 mm) were
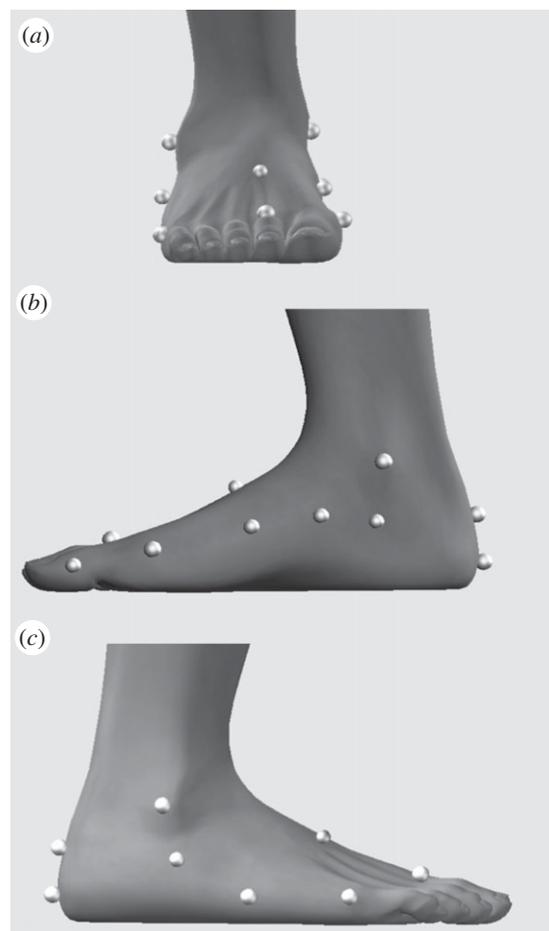
Figure 3. Multi-segment foot model marker locations. Retro-reflective skin markers for three-dimensional motion capture were applied to the right foot of each subject over defined anatomical landmarks in order to create a multi-segment foot model [1]. The figure depicts views from the anterior (*a*), medial (*b*) and lateral (*c*) aspects of the right foot. Markers were attached to rigid plastic discs that were secured to the skin with double-sided adhesive tape.

placed on the skin of the right foot and ankle according to a multi-segment foot model developed to describe rear-, mid- and fore-foot motion [1] (figure 3). This model [1] has been designed to describe motion of the LA and has been shown to have a high inter- and intratester repeatability in healthy adults [20]. Marker trajectory and force data were collected synchronously at 200 Hz using a four camera motion-capture system (Vicon MX, Vicon Motion Systems, Oxford, UK) and the previously described force platform. All marker trajectories and force plate data were processed using VISUAL 3D (C-Motion Inc., Germantown, PA, USA) with the marker trajectories filtered using a 6 Hz, low pass, fourth-order Butterworth filter. Assumed rigid segments were created according to the previously described multi-segment foot model [1] including the calcaneus, mid-foot and metatarsals.

2.5. Data analysis
2.5.1. Muscle activation
Root mean square (r.m.s.) signal amplitude of the EMG data was calculated over the middle 3 s epoch of each 5 s loading increment in experiment 1. RMS amplitudes were normalized to the maximal occurring r.m.s. amplitude recorded over a 1 s epoch for each muscle across all loading trials.

2.5.2. Arch deformation and muscle lengths
The LA height was defined from the three-dimensional-motion data as the vertical height of the navicular marker from the

floor [21,22]. LA length was defined as the straightline distance between the markers located on the medial calcaneus and the head of the first metatarsal.

For experiment 1, LA height and muscle tendon unit (MTU) lengths were calculated over the same 3 s epochs as the EMG data, corresponding to each 25% loading increment. These values were normalized to the values recorded prior to any loading being applied to the rig. Thus, LA length and height and MTU length were expressed as changes relative to the unloaded posture.

For experiment 2, LA length and height prior to electrical stimulation (loading condition) and that occurring during stimulation (stimulated condition) were calculated for each loading condition (50% and 100% body mass). The peak values for the three stimulations recorded during each trial were averaged for each condition and normalized to the LA length and height recorded prior to the application of any load to determine the effect of load and stimulation.

MTU lengths for AH, FDB and QP were determined based on a geometrical model according to the multi-segment three-dimensional-motion data, by defining virtual markers corresponding to the origin, tether and insertion points for AH and FDB, in accordance with previous cadaveric descriptions for these muscles [11–13]. Origin, tether and insertion points were expressed as fixed locations on the bony segment to which they were attached, allowing estimation of changes in MTU length according to the motion of the rigid foot segments. A tether point (a point that the line of action of the muscle is constrained to pass through) was created for the AH muscle to represent the fascial encapsulation of this muscle that occurs posterior to the navicular bone, extending from the deltoid ligament [23]. This encapsulation serves as a pulley, changing the anatomical pathway for this muscle. Each MTU length was defined as the straightline distance from the origin to the insertion, via any tether points.

In order to provide detailed insights into the contribution of individual foot segments to the biomechanics of the LA owing to the application of load and muscle stimulation, segment angles for the calcaneus and metatarsals were calculated in the sagittal, frontal and transverse planes (experiment 2 only). Angular rotations of these segments were defined relative to the laboratory coordinate system ($+x$-lateral, $+y$-anterior, $+z$-up) and according to an x–y–z Cardan sequence of rotations, i.e. rotation about the x-axis—sagittal plane motion; rotation about the y-axis—frontal plane motion; rotation about the z-axis—transverse plane motion. For the purpose of aligning our findings with previous cadaveric and *in vivo* data, we termed rotation about the x-axis as extension (positive) and flexion, rotation about the y-axis as inversion (positive) and eversion, and z-axis rotations as adduction (positive) and abduction. Segment angles were normalized to unloaded segment angles that were recorded in the experimental position prior to the application of load, so that zero degrees about all axes represented the segment angle when the foot was unloaded. For each participant, mean angular rotations were calculated within the sagittal, frontal and transverse planes by creating an average of the angular path associated with the three stimulations in each task across a 2 s window from the onset of stimulation and continuing for 1.5 s following the cessation of the stimulation train. Joint angles were normalized and calculated for loading and stimulation conditions by applying the same method described for LA length and height.

2.5.3. Force measurements
Vertical ground reaction force (F_z) and centre of pressure (COP) in the anteroposterior (COP_{AP}) and mediolateral (COP_{ML}) directions were calculated from the ground reaction force and moment data which were low-pass filtered with a fourth-order 6 Hz Butterworth filter. During experiment 2, the COP position and F_z values were calculated prior to muscle stimulation, as well as the peak value

occurring during muscle stimulation. Centre of pressure and F_z values were averaged over the three stimulations for each muscle and condition using the same procedure described for the kinematic data.

2.6. Statistics
Group means for LA height, MTU length and EMG r.m.s. activity were calculated at each loading increment in order to describe how these variables change as loading increased (experiment 1). A two-way repeated measures ANOVA was used to determine the effect of loading (50% versus 100% body mass) and muscle stimulation on LA length, LA height, segment angles, COP and F_z for AH, FDB and QP muscles (experiment 2). Multiple comparison tests including Bonferroni corrections were applied as post hoc analysis between conditions when significant main effects were reported. Statistical differences were established at $p \leq 0.05$. Results are presented as mean $\pm$ s.e., unless otherwise stated.

3. Results
3.1. Experiment 1: response to loading
Intramuscular EMG data for the AH and FDB muscles were obtained from all nine participants, however, QP data were only obtained from five participants due-poor signal to noise quality. Mean unloaded lengths for the AH, FDB and QP MTUs were 168.8 ± 6.9, 153.3 ± 4.5 and 65.5 ± 3.9 mm, respectively.

The relationship between the external load applied to the leg and foot, and (i) change in LA height, (ii) change in AH, FDB and QP length, and (iii) AH, FDB and QP normalized EMG r.m.s. activity are shown in figure 4. With an increase in load, there was a reduction in LA height and a subsequent stretch in the MTUs of AH, FDB and QP. The load under which muscle activity could first be detected, or load threshold, was different for each muscle. Despite MTU lengthening, muscle activity was first evident when loading reached 50%, 75% and 100% of body mass for FDB, QP and AH, respectively. Beyond these individual muscle thresholds, there was a progressive increase in activation with increasing load for all muscles. LA height and the lengths of the AH, FDB and QP MTUs appeared to plateau around 125% body mass, whereas muscle activation continued to increase up to the highest load tested (150% body mass).

3.2. Experiment 2: response to stimulation
3.2.1. Longitudinal arch length and height
Mean unloaded LA length and height was 156.7 ± 18.2 and 53.5 ± 4.7 mm, respectively. The height and length of the LA was significantly influenced by loading and muscle stimulation for all muscles (all $p \leq 0.05$). The LA was significantly longer and lower when loaded with 100%, compared with 50% body mass ($p \leq 0.05$, figure 5). Individual stimulation of AH, FDB and QP muscles countered the LA deformation produced by the load, by reducing the length and increasing the height of the LA when loaded with both 50% and 100% body mass (all $p \leq 0.05$, figure 5).

The alterations in LA length and height described above occurred as a result of a series of rotations occurring in multiple segments of the foot. In order to provide additional insights into the biomechanics of LA deformation and the impact of the plantar intrinsic foot muscles on this process, we have described the motion of the calcaneus and metatarsal segments during the
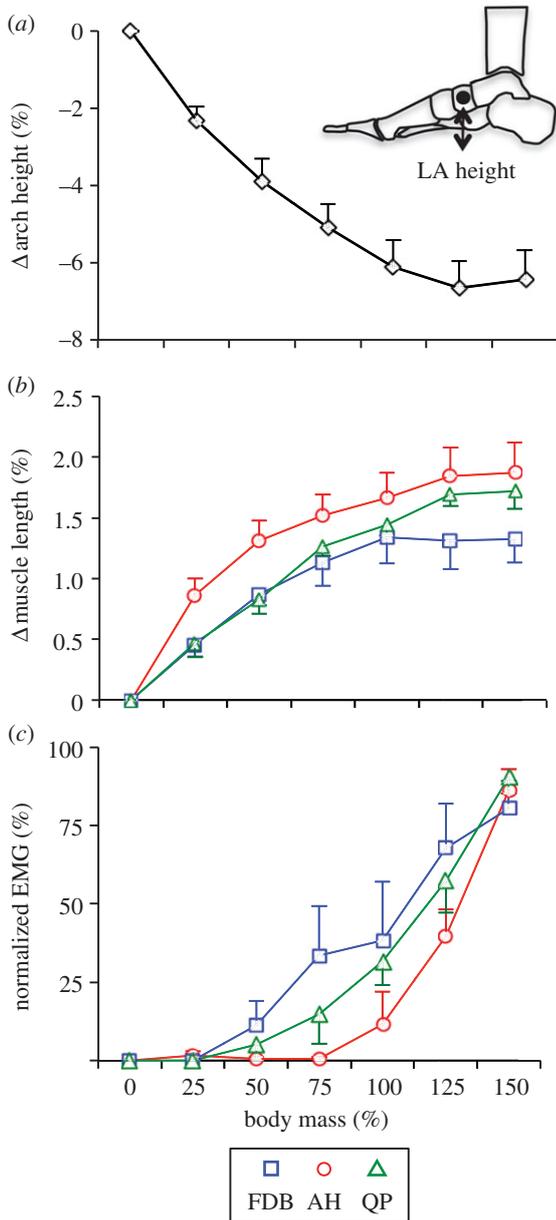
Figure 4. Group means $\pm$ s.d. for (a) change in longitudinal arch (LA) height, (b) change in muscle tendon unit length and (c) normalized electromyographic (EMG) root mean square (r.m.s.) plotted as a function of load applied to the thigh during the incremental loading task. For each participant, muscle length and arch height were normalized to the resting unloaded values. The EMG r.m.s. amplitude was normalized to the maximal value recorded during the 150% body mass trial. Open circles (red) represent abductor hallucis, open squares (blue) represent flexor digitorum brevis and open triangles (green) represent quadratus plantae muscle. (Online version in colour.)

Figure 5. (a) Diagram of the measurements of longitudinal arch (LA) length and height. (b) Group mean $\pm$ s.e. for LA length and height with 50% (open) and 100% (filled) body mass loading for abductor hallucis (AH, red), flexor digitorum brevis (FDB, blue) and quadratus plantae (QP, green) muscles. LA length and height values are shown in response to loading (squares) and stimulation (circles). Length and height of the LA are presented as a percentage change from the resting unloaded LA values (mean unloaded LA length = 156.7 $\pm$ 18.2 mm, mean unloaded LA height = 53.5 $\pm$ 4.7 mm). Stimulation of AH, FDB and QP resulted in a significant reduction in LA length and increase in LA height for all conditions (all $p \leq 0.05$). (Online version in colour.)

loading and stimulation tasks. These findings are explained below and a visual depiction can be found in figure 6.

3.2.2. Calcaneus motion

When loaded with 50% body mass, angular displacements of the calcaneus were observed in the sagittal (extension), frontal (eversion) and transverse (adduction) planes, with the orientation of the calcaneus remaining similar when load was increased to 100% of body mass (all $p > 0.05$, figure 7). Stimulation of AH produced extension, inversion and abduction of the calcaneus in the 50% body mass condition ($p \leq 0.05$) and inversion and abduction of the calcaneus in the 100% body mass condition ($p \leq 0.05$). Stimulation of FDB produced

inversion and abduction of the calcaneus in both 50% and 100% body mass conditions (all $p \leq 0.05$), whereas stimulation of QP produced abduction of the calcaneus in both 50% and 100% loading conditions (both $p \leq 0.05$).

3.2.3. Metatarsal motion

Under loads equivalent to 50% body mass, the metatarsal segment flexed (sagittal plane) and abducted (transverse plane), with these rotations increasing significantly when load was increased to 100% of body mass (all $p \leq 0.05$, figure 7). Individual stimulation of AH, FDB and QP significantly changed the orientation of the metatarsal segment, in the opposite direction to that observed with the application
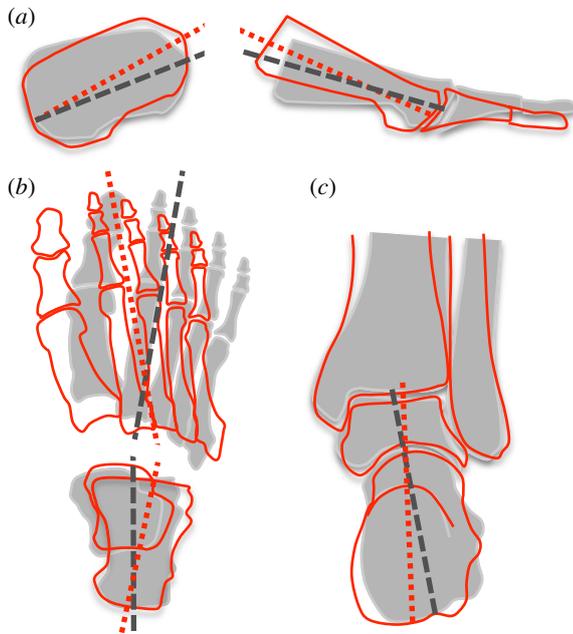
Figure 6. Depiction of foot motion changes occurring owing to stimulation of abductor halluces (AH). The position of the foot segments under load is represented by the grey-shaded image and the stimulated position is represented by the red outlined image. The movements include (a) calcaneal extension and metatarsal flexion in the sagittal plane (b) calcaneal abduction and metatarsal adduction in the axial plane and (c) calcaneal inversion in the frontal plane. This combination of segment movements lead to a reduction in length and an increase in height of the longitudinal arch. (Online version in colour.)

of load (all $p \leq 0.05$). Stimulation of AH produced flexion and adduction of the metatarsals, whereas stimulation of FDB and QP produced adduction of the metatarsals under loads of 50% and 100% of body mass (all $p \leq 0.05$).

3.2.4. Force measurements

The location of COP_{ML} or COP_{AP} remained unchanged in both loading conditions ($p > 0.05$). Stimulation of AH shifted the COP posteriorly and laterally for both 50% and 100% loading conditions (both $p \leq 0.05$), whereas stimulation of FDB and QP produced a significant posterior shift in the location of the COP for both loading conditions (both $p \leq 0.05$, figure 8).

Individual stimulation of AH, FDB and QP produced an increase in vertical force, in both the 50% (AH: 23.09 ± 8.7 N, FDB: 21.89 ± 13.2 N and QP: 20.43 ± 11.4 N, all $p \leq 0.05$) and 100% (AH: 22.73 ± 12.1 N, FDB: 20.97 ± 21.5 N and QP: 20.36 ± 21.8 N, all $p \leq 0.05$) body mass loading conditions.

4. Discussion

Our results demonstrate the importance of the intrinsic foot musculature in contributing to foot arch posture under physiological loads that would be exerted during tasks such as walking. We have shown that increased vertical loading resulted in significant LA length and height deformations, stretching of the arch musculature and increased electrical activity of the intrinsic foot muscles beyond specific load thresholds. This indicates that the intrinsic foot muscles respond to loading of the foot, however, their onset seems not to be mediated by stretch as MTU length increases were

evident, whereas EMG activity was notably absent at the lowest loading condition. Interestingly, foot deformation and muscle stretch plateaued at the highest loads; when muscle activity was still increasing. Our second experiment demonstrated that electrically induced contractions of individual intrinsic foot muscles (AH, FDB and QP), over and beyond their natural activity, can attenuate and even reverse LA arch deformation. Hence, these muscles have the capacity to stiffen the LA under load and could potentially account for the plateau in arch deformation observed at higher loads.

The capacity for the arch of the human foot to compress when loaded, allowing for storage of elastic strain energy, was dubbed the 'foot spring' mechanism by Ker et al. [2]. They reported that energy was stored as elastic strain in the passive ligamentous structures located within the LA, such as the plantar aponeurosis and plantar ligaments. This process was shown to provide metabolic energy savings as well as structural support countering compression of the LA. The results of our initial experiment confirm that the intrinsic foot muscles also stretch in response to LA deformation, with activation of these muscles increasing at higher loads. Results from experiment 2 suggest that these muscles have the capacity to contribute and attenuate arch deformation during loading. Therefore, activation of the intrinsic foot muscles with load may have the potential to provide a buttressing effect in parallel to that provided by the plantar aponeurosis. It appears that regulation of muscle activation may be contingent on loading demands, allowing forces generated from the intrinsic foot muscles to augment the contributions of the plantar aponeurosis once specific force or deformation thresholds are exceeded and potentially assisting in providing stabilization of the arch when encountered with excessive load.

A novel aspect of our study was the use of intramuscular electrical stimulation in addition to vertical loading to provide detailed insights into the biomechanical capability of the three largest plantar intrinsic foot muscles: AH, FDB and QP. Our data revealed that individual activation of AH, FDB and QP was sufficient to produce forces large enough to induce angular displacement of the calcaneus (extension, inversion and abduction) and metatarsals (flexion and adduction), which reduced the initial loading deformation by reducing LA length and increasing LA height. A conceptual figure demonstrating the general movement that occurs when the AH muscle is stimulated is shown in figure 6.

Despite the similar effect that individual muscle stimulations had on overall LA motion, differences did exist between muscles and the axis in which each muscle exerted mechanical influence on the calcaneal and metatarsal segments. The AH has the largest physiological cross-sectional area (PCSA) of the plantar intrinsic foot muscles [11,12] and stimulation of this muscle produced the most pronounced alterations in segment angles in all anatomical planes, including extension, inversion and abduction of the calcaneus, with flexion and adduction of the metatarsals. The FDB and QP have smaller PCSAs than AH [11,12] and, for the submaximal stimulation intensity used here, only exerted significant influence in the frontal (calcaneal inversion) and transverse (calcaneal abduction and metatarsal adduction) planes. The AH is also the most medially located of the three muscles investigated [13], therefore compared with FDB and QP, it may possess a greater moment arm over the joints of the LA, thereby giving it the possibility to produce larger torques and therefore greater segmental motion.
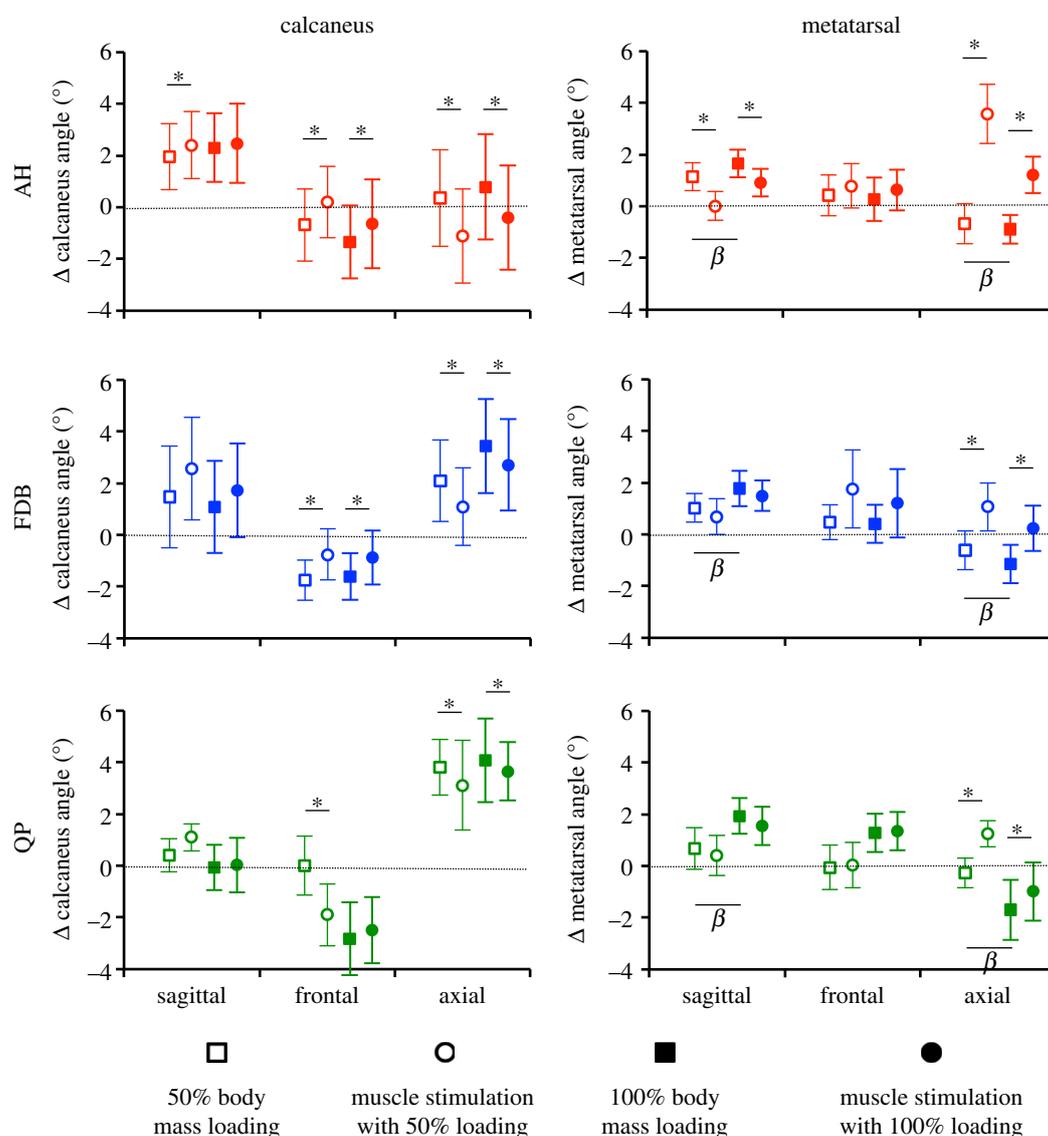
Figure 7. Changes in calcaneal and metatarsal segment angles owing to passive loading and intrinsic foot muscle stimulation. Group means ± s.e. for changes in calcaneal and metatarsal segment angles owing to loading, 50% (open) and 100% (filled) body mass as well as the subsequent changes in segment angles occurring with stimulation of abductor hallucis (AH, red), flexor digitorum brevis (FDB, blue) and quadratus plantae (QP, green) muscles. Segment angles are shown in response to loading (squares) and stimulation (circles). Angular rotations are defined relative to the laboratory coordinate system (x-lateral, y-anterior, z-upward) and according to an x−y−z Cardan sequence of rotations, with extension−flexion (positive extension) as the rotation about the x-axis, inversion−eversion (positive inversion) as the rotation about the y-axis and abduction−adduction (positive adduction) as the rotation about the z-axis. Segment angles are normalized to the seated, unloaded segment angle, such that zero degrees equals the unloaded segment angle for all axes. β indicates significant effect of load (100% versus 50% body mass) on segment angle. Asterisk indicates significant change in segment angle owing to muscle stimulation. (Online version in colour.)

Stimulation of the individual plantar intrinsic foot muscles produced angular displacement of the calcaneus and metatarsal segments which led to a reduction in arch length and an increase in arch height. Given that the applied downward load was constant during our muscle stimulations, a reduction in length of the LA indicates an overall increase in LA stiffness (reduced deformation for the same load). This may provide an explanation for the findings of Carravaggi et al. [8], Bates et al. [10] and Pataky et al. [9] who have suggested that active contractile mechanisms may provide substantial contributions to regulation of the stiffness of the LA. The presence of an active force generating element in parallel with a passive elastic element may help in both attenuation of impact forces and the generation of sufficient stiffness to transmit forces from the leg for effective forward propulsion [5]. Active stiffening of the LA may occur in a feedback or feed-forward manner in response to known or unknown variations in surface or loading demand, with the

intrinsic foot muscles contributing either negative or positive work in order to provide transient adjustments in stiffness, in addition to that provided by the passive structures [2–4,6]. This mechanism may contribute additional positive work, as required to provide postural stability [18] and aid in the transfer of ankle plantarflexion moments during gait and possibly generate additional positive power during propulsion [24].

A recent paper by Kelly et al. [18] used intramuscular EMG to describe the activation patterns of the plantar intrinsic foot muscles during various standing balance tasks and reported highly correlated intermuscular activation with medial postural sway. This study was unable to determine whether these relatively small muscles were capable of generating sufficient force to alter COP position and thus influence posture. In this study, we have extended the findings of Kelly et al. [18] by confirming that even individual activation of these muscles is capable of shifting the COP location, and as such could play
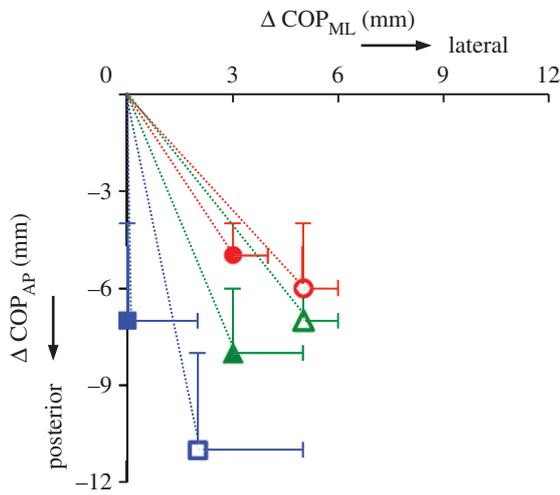
Figure 8. Changes in centre of pressure (COP) position owing to intrinsic foot muscle stimulation. Mean $\pm$ s.e. for COP in the mediolateral (COP_{ML}, x-coordinate) and anteroposterior (COP_{AP}, y-coordinate) directions occurring owing to electrically evoked contractions in abductor hallucis (red circle), flexor digitorum brevis (blue square) and quadratus plantae (green triangle) with both 50% (open) and 100% (filled) loading conditions. Changes in COP position were calculated by subtracting the COP position immediately prior to stimulation from the subsequent maximum COP displacement that occurred during muscle stimulation, such that 0,0 (x,y) represents the COP position prior to muscle stimulation, for all conditions. Stimulation of AH, FDB and QP produced significant changes in COP position in both loading conditions (all $p \leq 0.05$). (Online version in colour.)

a part along with other lower limb muscles in balance control. An interesting finding from this study was that stimulation of the intrinsic foot muscles resulted in a posterior shift in COP. This may be due to the shortening of the LA, predominantly arising from its distal end, and thus a posterior displacement in COP. In this study, we have largely eliminated postural influences by recording data from subjects in a seated position with weights loaded on to their knees, in order to simulate the loads applied during standing, in the absence of postural sway. This may help to explain the divergence in results between this study and that of Kelly et al. [18] who found no correlation between COP_{AP} and intrinsic foot muscle activation, as any relationship between COP_{AP} and muscle activity may have been hidden by the moments produced by the significantly larger soleus and gastrocnemius muscles.

There are some limitations to the approach used here in attempting to understand the capacity of the intrinsic foot muscles to adapt foot stiffness under load. During the incremental loading task, QP muscle activation was not able to be collected from all participants. In four participants, muscle activation could not be distinguished from background noise. This may have been due to the unstable nature of recordings from this small muscle, or conversely, it may also be due to a lack of activation within QP under the

loading conditions produced in this study. Additionally, for experiment 2, we have not made direct statistical comparison between muscles, as we are uncertain whether all muscles were contracting with the same relative intensity. Normalization of the stimulation intensity across muscles could be achieved by evoking a supramaximally stimulated contraction, however, this was not attempted due to the risk of damage to muscle tissue, discomfort and the increased risk of the stimulation current spreading to other nearby muscles which would confound the results. It is also difficult to ascertain what the summative effect of muscle activation might be in terms of both kinematics and kinetics as we did not simultaneously stimulate all three muscles. Our prediction is, however, that simultaneous activation (which is likely to be the physiological normality in walking and running) would increase the overall effect with an even greater increase in LA height and reduction of LA length. It must also be acknowledged that as we did not record EMG from these muscles during the evoked muscle stimulations, we cannot verify that they were quiescent during these tasks. In fact, based on the results of experiment 1, it is likely that these muscles may been active in the 100% body mass loading condition and as such our measures may have been influenced by a low level of background activation. Finally, we relied on skin-mounted markers to determine changes in LA height and length as well as movement of calcaneus and metatarsal segments. This approach is likely to underestimate some of the motion of the mid-foot during walking [25], however, we are confident that the general movement directions measured are consistent with what actually occurred during loading and muscle stimulation. The model we have used has been specifically designed to examine LA biomechanics, and has been shown to have high repeatability [20]. In our measures, the movement of the foot segments is limited compared with walking and hence the contribution of factors such as skin movement relative to the foot segments is also more limited and changes in marker position are likely to represent motion of foot rather than that of the skin.

In summary, our initial experiment has shown that the intrinsic foot musculature stretched in a similar manner to that of the plantar aponeurosis in response to LA deformation, whereas muscle activation increased considerably as loads increased beyond certain threshold loads for each muscle. Our following experiment has shown that activation of the plantar intrinsic foot muscles under load produced significant alterations in metatarsal and calcaneus segment angles, which countered the deformation occurring owing to the initial load and ultimately increased LA stiffness. This active arch buttressing mechanism may have important implications for how forces are transmitted during locomotion and postural activities. Future studies should examine the influence of the plantar intrinsic foot muscles on LA biomechanics during dynamic activities such as walking and running.

References

1. Leardini A, Benedetti MG, Berti L, Bettinelli D, Nativo R, Giannini S. 2007 Rear-foot, mid-foot and fore-foot motion during the stance phase of gait. Gait Posture 25, 453–462. (doi:10.1016/j.gaitpost. 2006.05.017)

2. Ker RF, Bennett MB, Bibby SR, Kester RC, Alexander RM. 1987 The spring in the arch of the human foot. Nature 325, 147–149. (doi:10.1038/325147a0)

3. Erdemir A, Hamel AJ, Fauth AR, Piazza SJ, Sharkey NA. 2004 Dynamic loading of the plantar

aponeurosis in walking. J Bone Joint Surg. Am. A 86, 546–552.

4. Hicks J. 1954 The mechanics of the foot: II. The plantar aponeurosis and the arch. J. Anat. 88, 25.

5. Vereecke EE, Aerts P. 2008 The mechanics of the gibbon foot and its potential for elastic energy storage during bipedalism. *J. Exp. Biol.* **211**, 3661–3670. (doi:10.1242/jeb.018754)

6. Caravaggi P, Pataky T, Goulermas JY, Savage R, Crompton R. 2009 A dynamic model of the windlass mechanism of the foot: evidence for early stance phase preloading of the plantar aponeurosis. *J. Exp. Biol.* **212**, 2491–2499. (doi:10.1242/jeb.025767)

7. Donatelli R. 1985 Normal biomechanics of the foot and ankle. *J. Orthop. Sports Phys. Ther.* **7**, 91–95. (doi:10.2519/jospt.1985.7.3.91)

8. Caravaggi P, Pataky T, Günther M, Savage R, Crompton R. 2010 Dynamics of longitudinal arch support in relation to walking speed: contribution of the plantar aponeurosis. *J. Anat.* **217**, 254–261. (doi:10.1111/j.1469-7580.2010.01261.x)

9. Pataky TC, Caravaggi P, Savage R, Parker D, Goulermas JY, Sellers WI, Crompton RH. 2008 New insights into the plantar pressure correlates of walking speed using pedobarographic statistical parametric mapping (pSPM). *J. Biomech.* **41**, 1987–1994. (doi:10.1016/j.jbiomech.2008.03.034)

10. Bates KT *et al*. 2013 The evolution of compliance in the human lateral mid-foot. *Proc. R. Soc. B* **280**, 20131818. (doi:10.1098/rspb.2013.1818)

11. Kura H, Luo ZP, Kitaoka HB, An KN. 1997 Quantitative analysis of the intrinsic muscles of the foot. *Anat. Rec.* **249**, 143–151. (doi:10.1002/(SICI)1097-0185(199709)249:1<143::AID-AR17>3.0.CO;2-P)

12. Ledoux WR, Hirsch BE, Church T, Caunin M. 2001 Pennation angles of the intrinsic muscles of the foot. *J. Biomech.* **34**, 399–403. (doi:10.1016/S0021-9290(00)00194-9)

13. Tosovic D, Ghebremedhin E, Glen C, Gorelick M, Brown JM. 2012 The architecture and contraction time of intrinsic foot muscles. *J. Electromyogr. Kinesiol.* **22**, 930–938. (doi:10.1016/j.jelekin.2012.05.002)

14. Thibodeau GA, Patton KT. 2007 *Anatomy and physiology*, 6th edn. St Louis, MO: Mosby Elsevier.

15. Basmajian JV, Stecko G. 1963 The role of muscles in arch support of the foot. *J. Bone Joint Surg. Am.* **45**, 1184–1190.

16. Mann R, Inman VT. 1964 Phasic activity of intrinsic muscles of the foot. *J. Bone Joint Surg. Am.* **46**, 469–481.

17. Gray EG, Basmajian JV. 1968 Electromyography and cinematography of leg and foot ('normal' and flat) during walking. *Anat. Rec.* **161**, 1–15. (doi:10.1002/ar.1091610101)

18. Kelly LA, Kuitunen S, Racinais S, Cresswell AG. 2012 Recruitment of the plantar intrinsic foot muscles with increasing postural demand. *J. Clin. Biomech.* **27**, 46–51. (doi:10.1016/j.clinbiomech.2011.07.013)

19. Tokuno CD, Carpenter MG, Thorstensson A, Garland SJ, Cresswell AG. 2007 Control of the triceps surae during the postural sway of quiet standing. *Acta Physiol.* **191**, 229–236. (doi:10.1111/j.1748-1716.2007.01727.x)

20. Caravaggi P, Benedetti MG, Berti L, Leardini A. 2011 Repeatability of a multi-segment foot protocol in adult subjects. *Gait Posture* **33**, 133–135. (doi:10.1016/j.gaitpost.2010.08.013)

21. Nielsen RG, Rathleff MS, Simonsen OH, Langberg H. 2009 Determination of normal values for navicular drop during walking: a new model correcting for foot length and gender. *J. Foot Ankle Res.* **2**, 12. (doi:10.1186/1757-1146-2-12)

22. Hageman ER, Hall M, Sterner EG, Mirka GA. 2011 Medial longitudinal arch deformation during walking and stair navigation while carrying loads. *Foot Ankle Int.* **32**, 623–629. (doi:10.3113/FAI.2011.0623)

23. Wong YS. 2007 Influence of the abductor hallucis muscle on the medial arch of the foot: a kinematic and anatomical cadaver study. *Foot Ankle Int.* **28**, 617–620. (doi:10.3113/FAI.2007.0617)

24. Zelik KE, Kuo AD. 2010 Human walking isn't all hard work: evidence of soft tissue contributions to energy dissipation and return. *J. Exp. Biol.* **213**, 4257–4264. (doi:10.1242/jeb.044297)

25. Nester C, Jones RK, Liu A, Howard D, Lundberg A, Arndt A, Lundgren P, Stacoff A, Wolf P. 2007 Foot kinematics during walking measured using bone and surface mounted markers. *J. Biomech.* **40**, 3412–3423. (doi:10.1016/j.jbiomech.2007.05.019)